AWESW2022
21st Australasian Wind Engineering Society Workshop
2 – 3 February, 2023

Assessment of Building-Generated Windshear at Airports

Ben Malin[1]

[1]Mott MacDonald, Adelaide, SA, 5000, Australia - ben.malin@mottmac.com.

ABSTRACT

Building-generated windshear is a known hazard to landing aircraft. In Australia, buildings constructed in the vicinity of airport runways must be assessed for this risk following the methodology in the National Airports Safeguarding Framework (NASF) Guideline B. The Guideline offers a simplified tabular building-induced wind speed deficit (BWD) calculation procedure.
A case study is presented of a warehouse building constructed in proximity to the runway of an Australian airport, with dimensions for which the BWD table is not applicable. The results of the NASF BWD calculation are compared against two alternative desktop procedures, and a CFD model. For the studied building, the alternate methods and RANS simulations predict similar BWD but are all far more conservative than the more sophisticated IDDES model.

1. Introduction

During strong winds, buildings in the vicinity of airport runways produce a turbulent wake which can interfere with landing aircraft. As an aircraft passes from the freestream through this turbulent wake, it may experience a sudden change in the apparent crosswind, referred to as building-generated windshear. To mitigate this hazard, new buildings near airports which fit certain criteria must be assessed for the strength and frequency of the windshear they are expected to produce across an airport's runways, following the recommendations and criteria in Guideline B (Department of Infrastructure and Transport, 2018) of the National Airport Safeguarding Framework (NASF).

Guideline B assesses windshear hazard in terms of mean building-induced wind speed deficit (BWD), the difference between an undisturbed wind and the wind in the wake of a building. The guideline provides a table-based (reproduced in Table 1) desktop method for assessing the BWD of a geometrically simple isolated building when wind is flowing perpendicular to its façade. For a given point downstream, generally the runway centerline, the table can be interpolated to determine the expected BWD as a fraction of the wind velocity at the roof height of the building, V_H.

Table 1. NASF Guideline B BWD assessment table (Department of Infrastructure and Transport, 2018)

BWD	**Width / Height**				
	1	**2**	**4**	**6**	**8**
0.48 V_H	1.7 H	3.4 H	6.5 H	9.5 H	12.5 H
0.35 V_H	2.2 H	4.2 H	8 H	11.5 H	15 H
0.22 V_H	3 H	5.5 H	10 H	14 H	18 H
0.11 V_H	5 H	9 H	17 H	24.5 H	32 H

One issue with this table is that airports often feature warehouse type buildings with large W/H ratios which lie outside the applicable range of this table. This work presents a case study of one such building, proposed for construction adjacent to the runway of an Australian airport. It has been represented as a simple box, with key properties summarized in Table 2. The resulting BWD from the Guideline B table is compared against two alternative BWD calculation procedures, as well as against a computational fluid dynamics (CFD) model of the building developed in OpenFOAM.

Table 2. Case study key parameters

Dimensions	106m (W) x 36m (D) x 10m (H) (W/H = 10.6)
Distance to runway	150m
Upstream roughness length, z_0	0.2m

2. Wake Deficit Calculation – Desktop Methods

The tabular methodology provided in Guideline B is based on the handbook of Leene et al. (1990). Wake profiles behind simple geometries (wall, porous blockage, rectangular building) are provided based on wind tunnel experiments, with a set of correction factors to account for different dimensions, terrain roughness, wind directionality and end effects. Based on the downstream distance to the runway, the expected BWD can be determined through interpolation of the provided wake profiles. This technique, referred to as the reference building method, has been used to calculate the BWD of the warehouse building in section 4.1.

The handbook also compares the empirical approach against the approach of Counihan et al. (1974), who derived a dimensionless analytical expression for the wake deficit behind an infinite two-dimensional fence. This analytical expression was later improved by Perera (1981), provided below:

$$\eta = \frac{z}{H} \cdot \left[\frac{1}{K\frac{X}{H}}\right]^{\frac{\ln\left(\frac{z}{z_0}\right)}{1+2\ln\left(\frac{z}{z_0}\right)}}, \ \ where \ \ K = \frac{2\kappa^2}{\ln\left(\frac{H}{z_0}\right)}, \ \ \kappa = 0.41 \quad (1)$$

$$\widetilde{U} = 9.75\eta \cdot e^{-0.67\eta^{1.5}} \quad (2)$$

$$C_B = 1 - \frac{\widetilde{U}}{\frac{X}{H} \cdot \frac{\ln(z/z_0)}{\ln(H/z_0)}} \quad (3)$$

$$BWD = (1 - C_B)V_{0,z} \quad (4)$$

Where η and $\widetilde{U}$ are the non-dimensional height and velocity respectively, C_B is the velocity reduction factor, z_0 is the aerodynamic roughness length, X is the downstream distance, H is the building height, and $V_{0,z}$ is the undisturbed mean velocity at height z. The non-dimensional wake profile is plotted below in Figure 1.

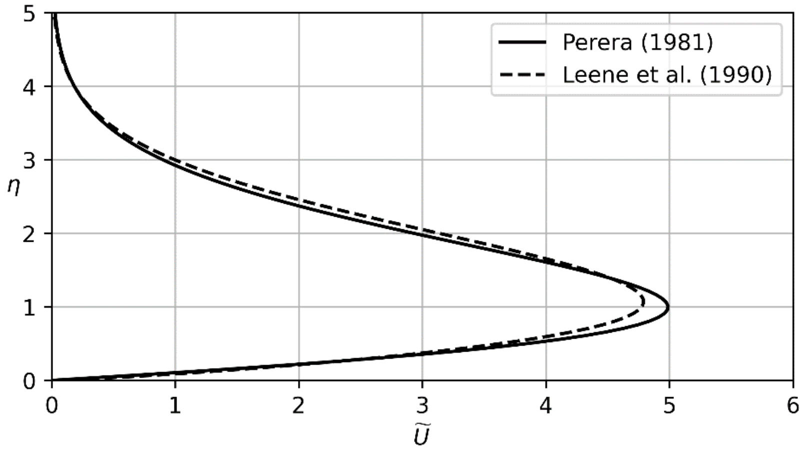

Figure 1. Non-dimensional wake deficit downstream of a 2D obstacle[1]

[1] The handbook of Leene et al. uses a Weibull function to approximate the velocity profile, but the function appears to be incorrect by a factor of two. When this error is corrected, the resulting curve matches Figure 18 in the handbook, and is close to the curve of Perera.

3. Wake Deficit Calculation – Computational Modelling

As an alternative to the desktop calculation methods, wind tunnel or computational modelling can be used to estimate the downstream wind shear. Modelling can provide a more accurate estimate of BWD, accounting for the detailed geometry of a building and its surroundings.

A key consideration when undertaking computational wind modelling is the choice of turbulence model. Reynolds Averaged Navier-Stokes (RANS) are known to under-predict turbulence generation in regions of flow separation over the building, and hence over-predict the strength and extent of the building wake (Blocken, 2011). By contrast, Large-Eddy Simulations (LES) are known to be far superior for modelling separated flows but are much more computationally expensive. In this work a RANS simulation using $k-\omega$SST (Menter 1993) has been compared with a Detached Eddy Simulation (DES), a hybrid technique that uses LES through most of the domain, and a RANS solution close to the wall to reduce the required mesh refinement. The Improved Delayed Detached Eddy Simulation (IDDES) version of the $k-\omega$SST model has been used in this case (Gritskevich et al. 2012).

The simulation mesh and domain extents are shown in Figure 2, which produce a blockage ratio of 0.44%. Refinement regions are used to improve resolution of the turbulent wake, and inflation layers are used to produce a mean Y+ at the building of approximately 400, as is appropriate when using a wall function approach.

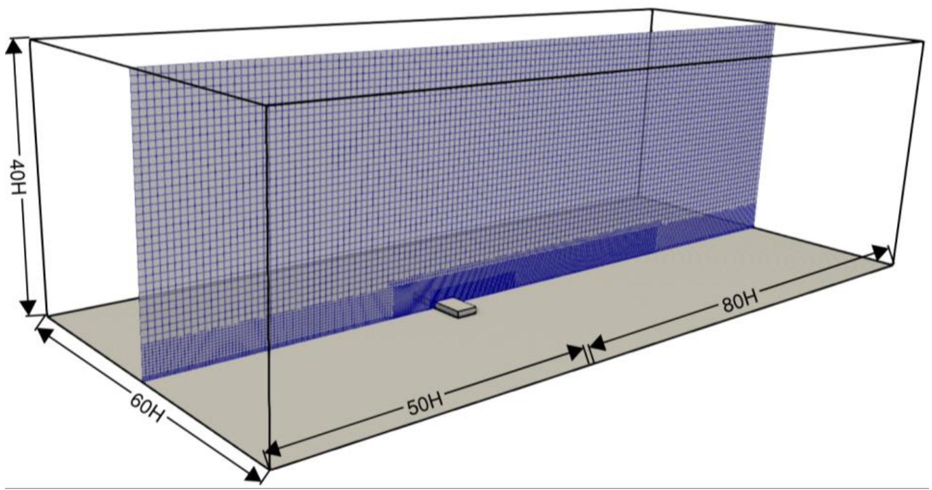

Figure 2. CFD simulation domain and mesh refinement

For the RANS simulation, atmospheric boundary layer (ABL) boundary conditions were implemented following the recommendations of Richards and Hoxey (1993), including the application of appropriate shear stress on the top boundary. A slip condition was used for the lateral boundaries, a roughness length rough wall function was used for the ground, and a smooth wall function was used for the building. The model is solved using OpenFOAM's steady-state incompressible solver, simpleFoam.

Setup of the DES case is similar to the RANS, with the primary modification being that a mean velocity inlet is no longer suitable. To produce flow with the appropriate statistics, the Divergence Free Spectral Representation (Melaku & Bitsuamlak 2021) method has been used to synthesise eddies at the inlet. A slip condition is used for the top boundary, and the model is solved with the unsteady incompressible pimpleFoam solver. Following a start-up period to allow the flow to reach an equilibrium, the wind velocity is sampled and averaged over a 10-minute period.

4. Results

4.1 Desktop methods

Following the Guideline B calculation procedure, there is an immediate problem: A W/H ratio of 10.6 lies beyond the horizontal bounds of the table. In the Handbook of Leene et al. the correction factor which accounts for the W/H ratio scales linearly up to a ratio of 10, beyond which it remains constant. This behavior is assumed to also apply for the table, allowing extrapolation to higher W/H ratios. As the runway lies at a downstream distance of X/H = 15, the vertical bounds of the table are also exceeded. While the columns of the table do not follow a linear trend, in this case the downstream point of interest is only marginally outside of the column extents, so the error associated with linear extrapolation should be small. The maximum resulting wake deficit at the runway is thus found to be $BWD = 0.50V_H$

For the reference building method perpendicular flow is assumed, and end effects are neglected. The effective downstream length is then calculated as:

$$\frac{X_e}{H} = \frac{X}{H} \cdot \frac{1}{\lambda_w \cdot \lambda_r} = \frac{150\ [m]}{10\ [m]} \cdot \frac{1}{1.2 \cdot 1} = 12.5 \qquad (5)$$

Where the λ terms are correction factors for W/H ratio and terrain roughness. Unfortunately, for this configuration the reference building approach also requires the extrapolation of a non-linear trend as seen in Figure 3. It is estimated that the maximum C_B using this method is approximately 0.6, resulting in a maximum wake deficit of $BWD = 0.4V_H$. This is clearly an unreliable approach, particularly if the runway centerline is located where $C_B < 0.7$.

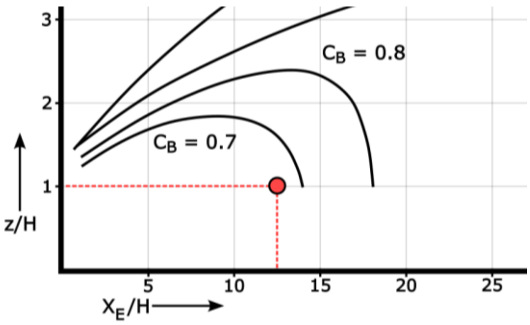

Figure 3. C_B at the effective downstream length (reproduction of Leene et al. Fig 24)

The wake deficit field produced by the non-dimensional wake profile method is plotted in Figure 4. At the runway centerline (at X/H = 15), the maximum C_B is found to be 0.64. Expressing relative to V_H, the maximum wake deficit at the runway is thus found to be $BWD = 0.33V_H$.

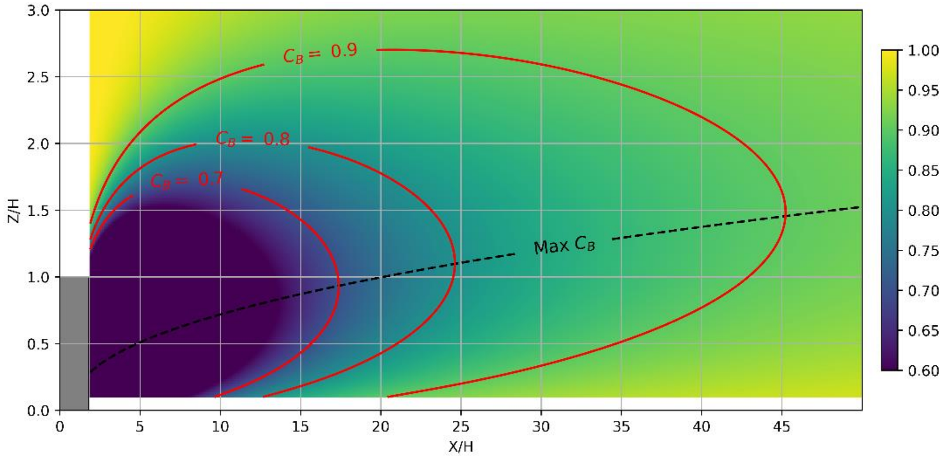

Figure 4. Expected velocity reduction factor using non-dimensional wake profile method

4.2 Computational modelling

The mean velocity for the RANS and IDDES simulations are plotted in Figure 5. In the RANS simulation, flow is fully detached across the entire roof of the building, and the wake extends a significant distance downstream. By contrast, the flow separation is seen to reattach to the building's roof in the IDDES case, and the wake returns to the freestream value much earlier. The resulting effect on the velocity reduction factor is clearly seen in Figure 6, where the RANS and IDDES results are compared against the non-dimensional wake method.

Note that the non-dimensional wake was conservatively assumed to begin from the leeward side of the building. However, based on these results and the underlying assumption of a fully detached flow, it would be appropriate and still conservative to take the windward façade as the beginning of the wake.

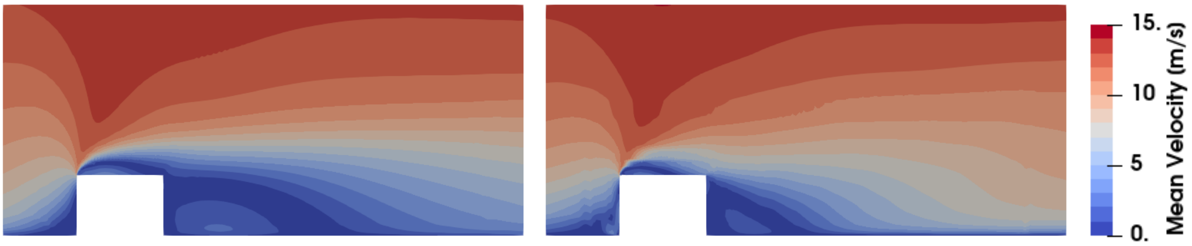

Figure 5. Comparison of mean velocity fields for RANS (left) vs IDDES (right). Images compressed horizontally

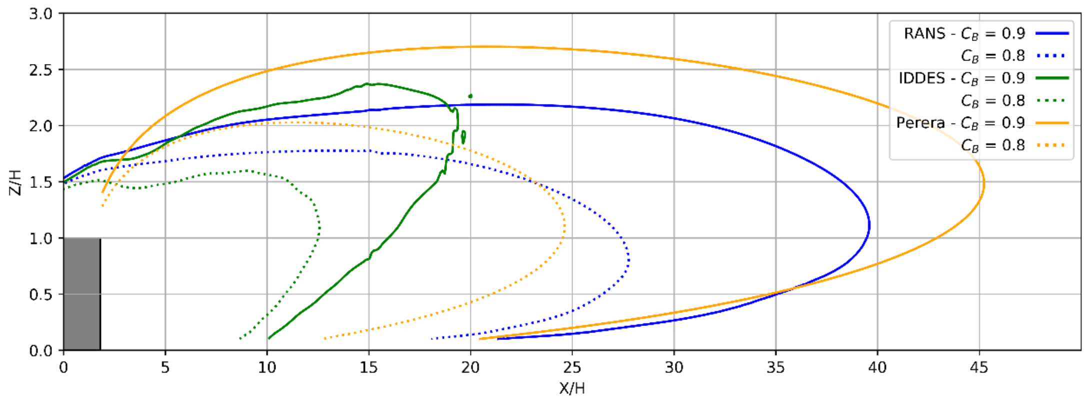

Figure 6. Comparison of velocity reduction factor predicted by the non-dimensional wake profile method and CFD models

A summary of the predicted BWD for each method is provided in Table 3. For this geometry, each of the methods are significantly more conservative than the IDDES simulation. The non-dimensional wake method in this instance produces a BWD closer to the IDDES result than even the RANS simulation.

Table 3. Precited BWD at the runway for each estimation methodology

Method	Guideline B Table	Reference Building[2]	Non-dimensional Wake	RANS	IDDES
Runway BWD	$0.5\ V_H$	$0.4\ V_H$	$0.348\ V_H$	$0.41\ V_H$	$0.16\ V_H$

The large difference between the RANS and IDDES results is likely exacerbated by the building geometry, where the flow can reattach in one simulation but not the other. Alternate geometry such as sufficiently peaked roofs or parapets, or a much different streamwise depth, might reduce this difference.

[2] Inaccurate due to extrapolation error as discussed in section 4.1

5. Conclusions

A variety of techniques for estimating the wind speed deficit in the wake of a rectangular building are compared in a case study of a warehouse building proposed for construction near the runway of an Australian airport. These techniques are investigated as possible alternatives for buildings which lie outside the applicable conditions for the tabular method in NASF Guideline B.

The reference building method shares the same deficiency for this application as the Guideline B tabular assessment, in that it cannot be appropriately applied to buildings with a high W/H ratio (10 or greater), particularly where the point of interest is located outside the applicable range of $C_B < 0.7$.

The desktop methods and the RANS simulation predict significantly larger wakes than the DES simulation, strengthening their role as highly conservative initial checks to inform more detailed modelling (DES/LES or wind tunnel). The BWD predicted by the DES model was less than half that of the other methods. The non-dimensional wake method predicts a similar wake profile to the RANS model, without the W/H ratio limitations of the other desktop methods.

In this case, the RANS simulation offered no benefit over the desktop non-dimensional wake method, particularly when considering the additional effort and computational expense.

References

Blocken, B., Stathopoulos, T., Carmeliet, J., & Hensen, J. L. M. (2011). Application of computational fluid dynamics in building performance simulation for the outdoor environment: An overview. Journal of Building Performance Simulation

Counihan, J., Hunt, J. C. R., & Jackson, P. S. (1974). Wakes behind two-dimensional surface obstacles in turbulent boundary layers. Journal of Fluid Mechanics, 64(3), 529–564.

Department of Infrastructure and Transport, (2018). Guideline B: Managing the Risk of Building Generated Windshear and Turbulence at Airports (National Airports Safeguarding Framework).

Gritskevich, M. S., Garbaruk, A. V., Schütze, J., & Menter, F. R. (2012). Development of DDES and IDDES Formulations for the k-ω Shear Stress Transport Model. Flow, Turbulence and Combustion, 88(3), 431–449.

Leene, J. A., Delaunay, D., & Jensen, A. G. (1990). Handbook on obstacle wake effects related to wind turbine siting (No. 90–117). Commission of the European Communities Directorate-General for Science, Research and Development.

Melaku, A. F., & Bitsuamlak, G. T. (2021). A divergence-free inflow turbulence generator using spectral representation method for large-eddy simulation of ABL flows. Journal of Wind Engineering and Industrial Aerodynamics, 212.

Menter, F. (1993). Zonal Two Equation k-w Turbulence Models For Aerodynamic Flows. 23rd Fluid Dynamics, Plasmadynamics, and Lasers Conference, Orlando, FL, U.S.A.

Perera, M. D. A. E. S. (1981). Shelter behind two-dimensional solid and porous fences. Journal of Wind Engineering and Industrial Aerodynamics, 8(1–2), 93–104.

Richards, P. J., & Hoxey, R. P. (1993). Appropriate boundary conditions for computational wind engineering models using the k-ε turbulence model. Computational Wind Engineering 1 (pp. 145–153). Elsevier.